Theoretical and Applied Fracture Mechanics 17 (1992) 61–68
Elsevier

Fracture behavior of beam cracked across reinforcement

Crescentino Bosco and Alberto Carpinteri

Department of Structural Engineering, Politecnico di Torino, 24 Corso Duca degli Abruzzi, 10129 Torino, Italy

Compliance change and crack tip stress intensity factor are applied to study the failure behavior of a reinforced beam with an edge crack in the matrix. Equal and opposite forces are applied to the crack surfaces to simulate the constraint of the reinforcement. Defined is a brittleness number that reflects the relative influence of the critical moment to trigger fracture and that to yield the reinforcement and hence the stability of crack propagation. Minimum reinforcement for stable failure corresponds to the condition when these two threshold moments are nearly equal. Numerical results are displayed graphically so that specific values of the loading and geometric parameters for a given failure behavior can be determined.

1. Introduction

The basic concept of fracture mechanics as applied to determine the failure behavior of columns and beams has received increasing attention with the realization that it could be applied to real situations [1]. The early studies on cracked columns [2,3] were followed by those on the cracking of reinforced concrete beams subjected to bending and tensile loads [4,5]. Repeated loadings [6] were also considered in examining the geometric scale effects of reinforced beams. This led to the determination of minimum reinforcement of high strength concrete beams [7,8]. It is, therefore, logical to develop the idea of cracking in reinforced structures where the matrix might behave linear elastically but the reinforcement could adopt a linear/elastic-perfect/plastic behavior.

The model adopted in this work again incorporates compliance with crack tip stress intensity. Included will be effect of matrix cracking across the reinforcement such that crack opening would be constrained. Results are discussed in connection with the ductile and brittle fracture behavior of the system.

2. Problem formulation

Consider the problem of a reinforced beam bent by moment M in Fig. 1 that contains an edge crack of length a. A pair of forces P on the crack simulates the constraint exerted by the reinforcement. Let $\Delta\phi_{MP}$ and $\Delta\delta_{PP}$ represent, respectively, the change in angle and crack opening displacement by the forces P at the points on the crack where they are applied, then the same quantities due to the bending

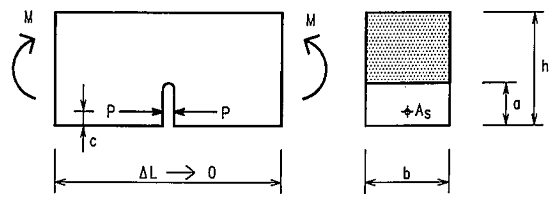

Fig. 1. Cracked element.

moments at M would be denoted by $\Delta\phi_{MM}$ and $\Delta\delta_{PM}$, respectively. Within the framework of linear analysis, superposition yields

$$\Delta\delta = \Delta\delta_{PM} + \Delta\delta_{PP} = \lambda_{PM}M - \lambda_{PP}P, \qquad \Delta\phi = \Delta\phi_{MM} + \Delta\phi_{MP} = \lambda_{MM}M - \lambda_{MP}P \tag{1}$$

where λ_{ij} $(i, j = M, P)$ are the compliances of the system.

If G denotes the strain energy release rate of the system, then the variation of the total potential energy is given by

$$\begin{aligned}\Delta W &= \int_0^c G_M \cdot b\ \mathrm{d}x + \int_c^a G_{(M+P)} \cdot b\ \mathrm{d}x \\ &= \int_0^c \frac{K_{\mathrm{I}M}^2}{E} b\ \mathrm{d}x + \int_c^a \frac{(K_{\mathrm{I}M} + K_{\mathrm{I}P})^2}{E} b\ \mathrm{d}x \\ &= \int_0^c \frac{K_{\mathrm{I}M}^2}{E} b\ \mathrm{d}x + \int_c^a \frac{K_{\mathrm{I}M}^2}{E} b\ \mathrm{d}x + \int_c^a \frac{K_{\mathrm{I}P}^2}{E} b\ \mathrm{d}x + 2\int_c^a \frac{K_{\mathrm{I}M}K_{\mathrm{I}P}}{E} b\ \mathrm{d}x \\ &= \int_0^a \frac{K_{\mathrm{I}M}^2}{E} b\ \mathrm{d}x + \int_c^a \frac{K_{\mathrm{I}P}^2}{E} b\ \mathrm{d}x + 2\int_c^a \frac{K_{\mathrm{I}M}K_{\mathrm{I}P}}{E} b\ \mathrm{d}x\end{aligned} \tag{2}$$

where b is the width of the beam. $K_{\mathrm{I}M}$ and $K_{\mathrm{I}P}$ are the stress intensity factors due to bending moment M and forces P, respectively.

The Clapeyron's Theorem yields

$$\Delta W = \tfrac{1}{2}M\Delta\phi_{MM} + \tfrac{1}{2}P\Delta\delta_{PP} + \tfrac{1}{2}(P\Delta\delta_{PM} + M\Delta\phi_{MP}) \tag{3}$$

Making use of the Betti's Theorem that gives

$$P\Delta\delta_{PM} = M\Delta\phi_{MP} \tag{4}$$

eqs. (2) and (3) can be reduced to the forms

$$\tfrac{1}{2}M\Delta\phi_{MM} = \int_0^a \frac{K_{\mathrm{I}M}^2}{E} b\ \mathrm{d}x, \qquad \tfrac{1}{2}P\Delta\delta_{PP} = \int_c^a \frac{K_{\mathrm{I}P}^2}{E} b\ \mathrm{d}x \tag{5}$$

such that

$$P\Delta\delta_{PM} = M\Delta\phi_{MP} = 2\int_c^a \frac{K_{\mathrm{I}M}K_{\mathrm{I}P}}{E} b\ \mathrm{d}x \tag{6}$$

Let the Mode I stress-intensity factor be expressed as [2,3]

$$K_{\mathrm{I}M} = Y_M(\xi)\frac{M}{bh^{3/2}} \tag{7}$$

in which $Y_M(\xi) = 6(1.99\xi^{1/2} - 2.47\xi^{3/2} + 12.97\xi^{5/2} - 23.17\xi^{7/2} + 24.80\xi^{9/2})$, for $\xi = a/h \leqslant 0.7$. Here, h is the height of the beam. Similarly, the Mode I stress intensity factor for the forces P applied at a distance c takes the form [9]

$$K_{\mathrm{I}P} = Y_{\mathrm{P}}(c/h, \xi)\frac{P}{b\sqrt{h}} \tag{8}$$

such that $\xi = a/h$ and

$$Y_P(c/h,\ \xi) = \frac{2}{\sqrt{\pi\xi}}\left\{\frac{3.52(1-c/a)}{(1-a/h)^{3/2}} - \frac{4.35-5.28\ c/a}{(1-a/h)^{3/2}} + \left[\frac{1.30-0.30(c/a)^{3/2}}{\left(1-(c/a)^2\right)^{1/2}} + 0.83 - 1.76\ c/a\right]\left[1-(1-c/a)a/h\right]\right\}$$

for $a/h < 1$ and $c/a < 1$.

Now, substitute eq. (7) into the first of eqs. (5) and divide the result by M^2 gives the compliance

$$\lambda_{MM} = \frac{2}{bh^2E}\int_0^{\xi} Y_M^2(\xi)\ \mathrm{d}\xi \tag{9}$$

with $M = 1$. In the same way, eq. (8) may be inserted into the second of eqs. (5) to yield the compliance

$$\lambda_{PP} = \frac{2}{bE}\int_{c/h}^{\xi} Y_P^2(c/h,\ \xi)\ \mathrm{d}\xi \tag{10}$$

for $P = 1$. Finally, eqs. (7) and (8) can be both put into eq. (6) rendering the mixed compliance

$$\lambda_{PM} = \lambda_{MP} = \frac{2}{bhE}\int_{c/h}^{\xi} Y_P(c/h,\ \xi)Y_M(\xi)\ \mathrm{d}\xi \tag{11}$$

with $M = 1$ and $P = 1$.

Numerical values of $Y_P(c/h,\ \xi)$ for $c/h = 0.05$, 0.10 and 0.15 and $\xi = a/h = 0.1, 0.2, \ldots, 0.7$ can be found in Fig. 2. For each c/h ratio, it is possible to show that Y_P tends to infinity for $\xi \to c/h^+$ and $\xi \to 1^-$. As a consequence, the K_{IP} factor gives a minimum for ξ between c/h and 1. The curve for $Y_M(\xi)$ with $\xi = a/h$ is also given. Functions $Y_P(c/h,\ \xi)Y_M(\xi)$ and $Y_M^2(\xi)$ with the related integrals are plotted in Figs. 3 and 4, respectively.

3. Crack surface constraint

The reinforcement exerts certain constraint on the crack by the closing forces

$$P = \sigma_s A_s \tag{12}$$

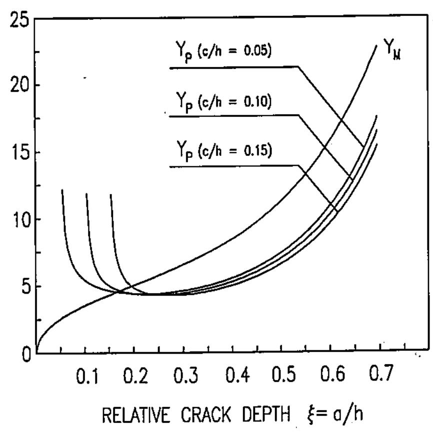

Fig. 2. Shape functions depending on relative crack depth.

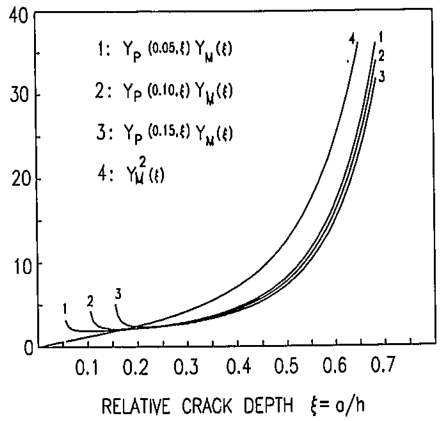

Fig. 3. Products of shape functions.

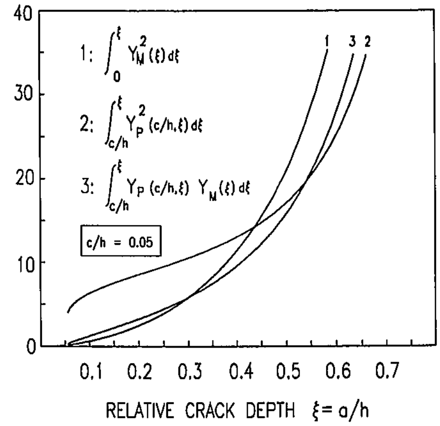

Fig. 4. Compliance functions.

with σ_s being the equivalent stress over the area A_s. Prior to yielding or slippage of the reinforcement, there is no local rotation of the cracked cross-section, i.e.,

$$\Delta\phi = \Delta\phi_{MM} + \Delta\phi_{MP} = \lambda_{MM} M - \lambda_{MP} P = 0 \tag{13}$$

This condition together with eqs. (9) and (11) determines P as

$$\frac{M}{Ph} = r^*(c/h, \xi) = \frac{\int_{c/h}^{\xi} Y_M(\xi) Y_P(c/h, \xi)\, d\xi}{\int_0^{\xi} Y_M^2(\xi)\, d\xi} \tag{14}$$

If $P_p = \sigma_{sp} A_s$ denotes the yield force and σ_{sp} the yield stress of an elastic-perfectly plastic reinforcement, then the plastic moment can be obtained from eq. (14) as

$$M_p = P_p h r^*(c/h, \xi) \tag{15}$$

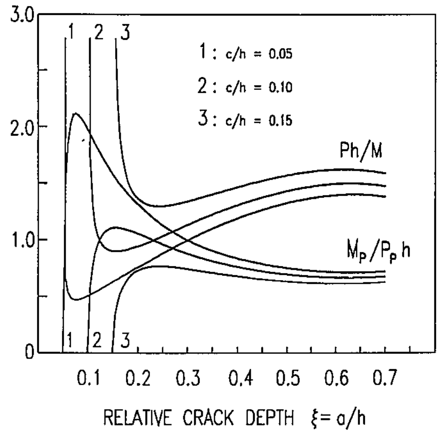

Fig. 5. Reinforcement constraint force versus crack depth.

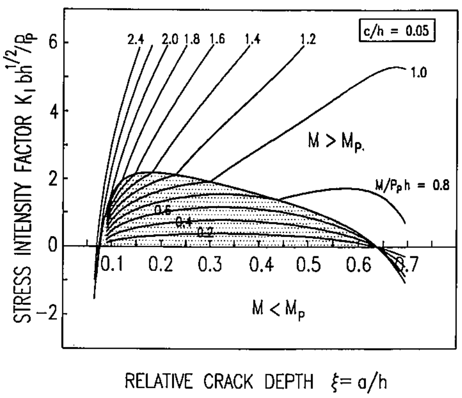

Fig. 6. Normalized stress intensity factor versus crack depth for varying M and $c/h = 0.05$.

The force P_p can also be regarded as the pull-out force of the reinforcement if such an action takes place before yielding.

Plotted in Fig. 5 are the force P in eq. (14) against $\xi = a/h$ for $c/h = 0.05$, 0.10 and 0.15. The values of $M_p/P_p h$ in eq. (15) are also shown.

4. Combined crack tip stress intensification

The stress intensity factors K_{IM} in eq. (7) and K_{IP} in eq. (8) can be added to yield

$$K_I(M, P) = K_{IM}(M) + K_{IP}(P) \quad \text{for } M < M_p \tag{16}$$

and hence for $P = P_p$, equation (16) applies to $M \geqslant M_p$ or

$$K_I(M, P) \to K_I(M, P_p) \quad \text{for } M \geqslant M_p \tag{17}$$

The force P and P_p in eqs. (16) and (17) may be eliminated by applying eqs. (14) and (15), respectively. It would therefore be understood that the combined stress intensity factor is

$$K_I = \begin{cases} K_I(M, P) & \text{for } M < M_p \\ K_I(M, P_p) & \text{for } M \geqslant M_p \end{cases} \tag{18}$$

Plotted in Figs. 6, 7 and 8 are, respectively, the values of K_I for $c/h = 0.05$, 0.10 and 0.15 as $\xi = a/h$ and $M/P_p h$ are varied. Two regions can be identified: one shaded corresponding to reinforcement not yielded and other unshaded. The shaded region in Fig. 6 terminates where horizontal line intersects at $\xi \simeq 0.075$ the curves for $M/P_p h \lesssim 2.11$ and at $\xi \simeq 0.63$ the curves for $M/P_p h \lesssim 0.71$. These two values of ξ are obtained by setting $K_I = 0$ in eq. (18) which is equivalent to letting

$$K_{IM} + K_{IP} = 0 \quad \text{or} \quad Y_M(\xi) - \frac{Y_P(c/h, \xi)}{r^*(c/h, \xi)} = 0 \tag{19}$$

Obviously, eq. (19) holds regardless of M. For $M/P_p h \lesssim 0.71$ and $\xi \lesssim 0.075$ or $\xi \gtrsim 0.63$, K_I could become negative. This means that crack would tend to close. A closer examination shows that for a relatively small moment $M/P_p h \lesssim 0.71$, the reinforcement could yield only for very small or very large ξ or crack depth.

Note that within the shaded region in Fig. 7, the K_I versus ξ curves for $M/P_p h \lesssim 0.95$ possess a maximum, say $K_{I\max}$ at $\xi \simeq 0.324$. This implies that crack would propagate with increasing K_I (unstable)

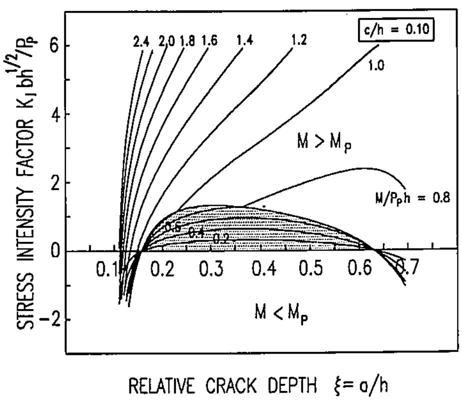

Fig. 7. Normalized stress intensity factor versus crack depth for varying M and $c/h = 0.10$.

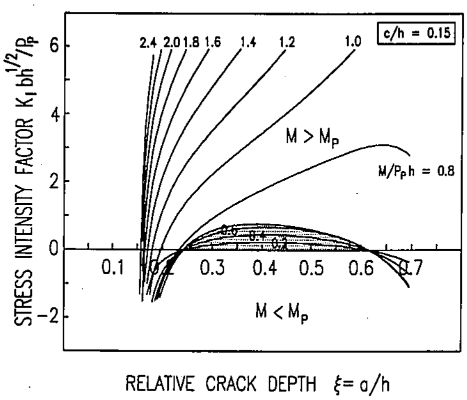

Fig. 8. Normalized stress intensity factor versus crack depth for varying M and $c/h = 0.15$.

or decreasing K_I (stable). In the unshaded region where the reinforcement has yielded, the maxima of the two curves for $M/P_p h = 0.8$ and 1.0 no longer occur at the same values of ξ and the curves for $M/P_p h > 1.1$ have no maxima.

Since the results in Fig. 7 for $c/h = 0.10$ and Fig. 8 for $c/h = 0.15$ are similar to those in Fig. 6, additional discussions are not necessary except to note that the size of the shaded region decreases with increasing c/h ratio.

5. Onset of matrix cracking

Let K_{Ic} denote the fracture toughness of the matrix material such that the onset of fracture corresponds to K_I in eq. (16) reaching K_{Ic}. Then the critical moment M_F can be found from the application of eqs. (7), (8) and (16)

$$K_{Ic} = \frac{M_F}{bh^{3/2}} Y_M(\xi) - \frac{P}{b\sqrt{h}} Y_P(c/h, \xi) \tag{20}$$

The above expression may be rearranged to read as

$$\frac{M_F}{bh^{3/2}K_{Ic}} = \frac{1}{Y_M(\xi)} + N_p \frac{Y_P(c/h, \xi)}{Y_M(\xi)} \tag{21}$$

in which N_p is defined as the brittleness number:

$$N_p = \frac{\sqrt{h}}{K_{Ic}} \left(\frac{P}{A}\right) \quad \text{with } P = \begin{cases} \sigma_{sp} A_s & \text{for } M_F \geqslant M_p \\ \sigma_s A_s & \text{for } M_F < M_p \end{cases} \tag{22}$$

where $A = bh$ is the cross sectional area of the beam. Remember that σ_{sp} is the yield stress of the reinforcement. Alternatively, eq. (14) for $M = M_F$ at fracture may be used in eq. (20) to give

$$\frac{M_F}{bh^{3/2}K_{Ic}} = \left[Y_M(\xi) - \frac{Y_P(c/h, \xi)}{r^*(c/h, \xi)} \right]^{-1} \tag{23}$$

The critical moment is seen to depend on the crack depth ξ for a given geometry and not on the brittleness number N_p.

Displayed graphically in Fig. 9 are the variations of normalized M_F in eq. (23) with ξ for $c/h = 0.05$ as N_p is varied. For $N_p \lesssim 0.46$, the condition $M_F > M_p$ prevails such that crack propagation occurs when

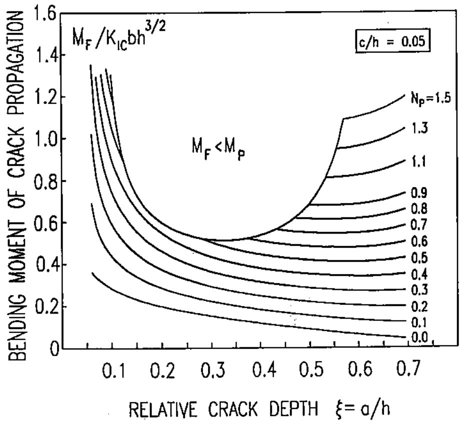

Fig. 9. Normalized critical moment versus crack depth for varying N_p and $c/h = 0.05$.

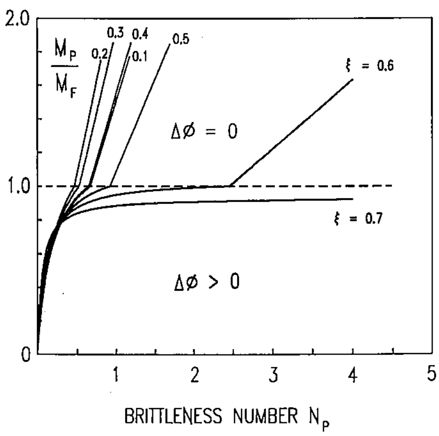

Fig. 10. Variations of threshold moment ratio M_p/M_F with N_p.

the reinforcement is in the yielded state. Those N_p = constant curves that do not intersect with the envelop $M_F = M_p$ tend to decrease with increasing ξ. The fracture moment of beams with low reinforcement and/or large cross sections would tend to decrease as the crack extends. This corresponds to unstable crack growth. Hence, cracking becomes stable if N_p is sufficiently high or when the beam cross section is relatively small and/or the reinforcement is relatively high.

6. Effect of reinforcement on fracture behavior

As discussed earlier, crack propagation can occur regardless of whether M_F is greater or smaller than M_p. That is, crack growth can take place with reinforcement yielding or without. The ratio M_p/M_F would be indicative of the effect of reinforcement on fracture behavior. To this end, eq. (20) can be arranged solving for $1/M_F$. Then, multiply one side of the resulting expression by M_p and the other side by $P_p h r^*(c/h, \xi)$ as given by eq. (15). With aid of the definition of N_p in eq. (22), it follows that

$$\frac{M_p}{M_F} = \frac{r^*(c/h, \xi) Y_M(\xi)}{N_p^{-1} + Y_p(c/h, \xi)\dfrac{P}{P_p}} \tag{24}$$

where $P = \sigma_{sp} A_s$ or $\sigma_s A_s$ depending on whether M_F is larger or smaller than M_p as defined in eq. (22).

A graphical representation of eq. (24) is given in Fig. 10 for different ξ and $c/h = 0.05$. Variations of M_p/M_F with N_p show that for $N_p \lesssim 0.46$, most of the results fall in the region $M_p > M_F$ except for large values of ξ where the curves fall below the line $M_p = M_F$. Two conditions of failure could occur:

- *Fracture before yield of reinforcement*. This occurs for $0.08 \lesssim \xi \lesssim 0.63$ and $N_p \gtrsim 0.46$ such that the beam fractures without local rotation of the cross section, i.e., $\Delta\phi = 0$.
- *Fracture after yield of reinforcement*. This corresponds to low values of N_p or large beam cross section and/or low strength reinforcement.

It is of interest in general to determine when M_F is nearly equal to M_p. This would correspond to the condition of minimum reinforcement [7,8] for stable failure upon reaching the critical moment.

7. Concluding remarks

Examined in this work is the influence of reinforcement on a crack in the matrix. A pair of closing forces is used to simulate the reinforcement constraint. Yielding of the reinforcement tends to alter this constraint and hence the onset of crack growth. Results are expressed in terms of the moments M_F and M_p corresponding to fracture initiation in the matrix and yield initiation in the reinforcement. Change in the failure behavior could also be reflected through a brittleness number N_p that weighs the relative magnitude of M_F and M_p through the reinforcement constraint stress in the elastic state σ_s and plastic state σ_{sp}.

For a rigid-plastic material with linear hardening, it is possible to obtain from eq. (13) the notation:

$$\Delta\phi = \lambda_{MM}(M - M_p) \quad \text{for } M > M_p \tag{25}$$

Unstable fracture coincides with the termination of hardening and is represented by the sudden drop on a plot of M versus $\Delta\phi$. The ligament of the specimen breaks off. Stable fracture would correspond to continuous hardening of the material [4,5] on the M versus $\Delta\phi$ curve. A transitional value of N_p, say N_{pc} can be defined from eq. (21) by letting $M_F = P_p h$ and knowing from eq. (22) that $P_p/b\sqrt{h}K_{Ic} = N_{pc}$. This yields immediately the relation

$$N_{pc} = \left[Y_M(\xi) - Y_P(c/h, \xi)\right]^{-1} \tag{26}$$

Stable fracture ($N_p > N_{pc}$) and unstable fracture ($N_p < N_{pc}$) can thus be identified simply with the geometric configuration of the specimen. These findings represent an improvement over the previous works [4,5] and could possibly provide better correlation of the data in [7,8].

Acknowledgements

The authors gratefully acknowledge the financial support of the National Research Council (C.N.R.) and the Department of University and Scientific and Technological Research (M.U.R.S.T.).

References

[1] G.C. Sih and A.M. Skudra (Eds.), *Failure Mechanics of Composites* (North-Holland: Amsterdam, 1985).
[2] H. Okamura, K. Watanabe and T. Takano, Applications of the compliance concepts in fracture mechanics, *ASTM STP 536* (1973) 423–438.
[3] H. Okamura, K. Watanabe and T. Takano, Deformation and strength of cracked member under bending moment and axial force, *J. Eng. Fract. Mech. 7* (1975) 531–539.
[4] A. Carpinteri, A fracture mechanics model for reinforced concrete collapse, *IABSE Colloquium on Advanced Mechanics of Reinforced Concrete*, Delft, 1981, pp. 17–30.
[5] A. Carpinteri, Stability of fracturing process in RC beams, *J. Struct. Eng. ASCE 110* (1984) 544–558.
[6] Al. Carpinteri and An. Carpinteri, Hysteretic behaviour of RC beams, *J. Struct. Eng. ASCE 110* (1984) 2073–2084.
[7] C. Bosco, A. Carpinteri and P.G. Debernardi, Minimum reinforcement in high-strength concrete, *J. Struct. Eng. ASCE 116* (1990) 427–437.
[8] C. Bosco, A. Carpinteri and P.G. Debernardi, Fracture of reinforced concrete: scale effect and snap-back instability, presented at the International Conference on Fracture and Damage of Concrete and Rock, July 4–6, 1988, Vienna, Austria, *J. Eng. Fract. Mech. 35* (4–5) (1990) 665–677.
[9] H. Tada, P. Paris and G. Irwin, *The Stress Analysis of Cracks Handbook* (Del Research Corporation: Hellertown, PA, USA, 1963) pp. 2.16–17.